https://doi.org/10.5194/egusphere-2022-225
Preprint. Discussion started: 27 April 2022

Building-scale flood loss estimation through enhanced vulnerability pattern characterization: application to an urban flood in Milano, Italy

Andrea Taramelli[1,2], Margherita Righini[1], Emiliana Valentini[3], Lorenzo Alfieri[4], Ignacio Gatti[1], Simone Gabellani[4]

[1]Istituto Universitario di Studi Superiori di Pavia (IUSS), Pavia, 27100, Italy
[2]Institute for Environmental Protection and Research (ISPRA), Roma, 00144, Italy
[3]Institute of Polar Sciences of the Italian National Research Council (ISP CNR), Roma, 00015, Italy
[4]CIMA Research Foundation, Savona, 17100, Italy

Correspondence to: Margherita Righini (margherita.righini@iusspavia.it)

Abstract. The vulnerability of flood-prone areas is determined by the susceptibility of the exposed assets to the hazard. It is a crucial component in risk assessment studies, both for climate change adaptation and disaster risk reduction. In this study, we analyse patterns of vulnerability for the residential sector in a frequently hit urban area of Milano, Italy. The conceptual foundation for a quantitative assessment of the structural dimensions of vulnerability is based on the modified Source-Pathway-Receptor-Consequence model. This conceptual model is used to improve the parameterization of the flood risk analysis describing: (i) hazard scenarios definition performed by hydraulic modelling based on past event data (Source estimation) and morphological features and land use evaluation (Pathway estimation); (ii) the exposure and vulnerability assessment which consists of recognizing elements potentially at risk (Receptor estimation) and event losses (Consequence estimation). The structural dimension of vulnerability is mapped at building level and used in loss estimation for the residential sector at meso and micro-scale. Results produces accurate estimates of the flood characteristics, with mean error in flood depths estimation in the range 0.2-0.3 m and provide a basis to obtain site-specific damage curves and damage mapping. Findings show that the nature of flood pathways varies spatially and is influenced by landscape characteristics and alters vulnerability spatial distribution and hazard propagation. At the mesoscale, the 'Continuous urban fabric' Urban Atlas 2018 land-use class with the occurrence of at least 80 % of soil sealing shows higher absolute damage values. At microscale, evidence demonstrated that even events with moderate magnitude in terms of flood depth in a complex urbanized area may cause more damage than it would expect.

1 Introduction

Flood risk is not stationary, it hinges on climate variability along with changes in vulnerability patterns of exposed elements (Lal et al., 2012). Climate change and socioeconomic developments strongly affect such natural dynamics, which include changes in the probability or intensity of hazards (Elmer et al., 2010; Cammerer et al., 2013; Cammerer and Thieken, 2013).

https://doi.org/10.5194/egusphere-2022-225
Preprint. Discussion started: 27 April 2022

Changes in flooding regimes associated with human-induced environmental variations and worsened climate change-related hazards are representative of socio-natural hazards. Vulnerability of elements at risk and the communities' adaptive capacity variations rely on socioeconomic developments entailing land use and changes in the exposure of people and assets (Hufschmidt et al., 2005; Taramelli et al., 2018; Bouwer et al., 2010; Meyer et al., 2013). The vulnerability is defined by the United Nations General Assembly (UNGA) as '*The conditions determined by physical, social, economic and environmental factors or processes which increase the susceptibility of an individual, a community, assets or systems to the impacts of hazards'* (UN Secretary-General, 2016). Therefore, vulnerability can be described as 1) multi-dimensional (e.g., physical, social-cultural, socio-economic, and environmental); 2) dynamic (i.e., vulnerability changes over time); 3) scale-dependent (i.e., vulnerability can be assessed at various spatial and temporal scales); 4) site-specific (i.e., the approach is defined by a specific location needs). The processes of vulnerability and risk assessment array from global and national quantitative methods to local-scale qualitative approaches (Lal et al., 2012). Indicators, indices, and probabilistic metrics are important measures and methods for vulnerability and risk analysis. However, qualitative approaches for assessing vulnerability need to be complemented with quantitative approaches to capture the full complexity and the various tangible and intangible dimensions of vulnerability (Lal et al., 2012; Morelli et al., 2021). Vulnerability can be seen as situation-specific, interacting with a hazard event to generate risk resulting from a complex set of drivers and interacting conditions (Cutter and Finch, 2008). Thus, it is essential to understand how vulnerability is generated, how it increases, and how it is distributed to effectively manage risk. Trends in vulnerability and exposure are major drivers of changes in disaster risk, and of impacts when risk is realized. Therefore, understanding the multifaceted nature of vulnerability and exposure is a prerequisite for determining how hazardous events contribute to the occurrence of disasters, and for implementing effective risk management strategies. The estimation of the structural dimension of vulnerability of flood-prone areas has proven to be key to analysing flood risk. Since the structural vulnerability is defined as the potential of a particular class of buildings or infrastructure facilities to be affected or damaged under a given flood intensity (Faella and Nigro, 2003), damage by flood hazard depends on the vulnerability of exposed buildings (Schanze J., 2006; Merz et al., 2010). The elements at risk level of vulnerability can be defined in manifold ways (UNISDR, 2017). Vulnerability information of buildings is commonly collected in the form of vulnerability curves, damage curves or vulnerability matrices, which imply the relationship between the levels of damage to a specific type of element at risk exposed to a given level of hazard intensity (e.g., water depth) (Nasiri et al., 2016). Developing accurate vulnerability curves is challenging, as they can be empirically built learning from past damage event for which information are freely available and accessible, or via numerical modelling (Roberts et al., 2009; Thieken et al., 2008). However, few studies describe the relation between potential losses and the structural factors (e.g., building type, quality, height, and material) (Taramelli et al., 2015). Reason for this are mainly related to the paucity of information related to building characteristics, the physical parameters of the damaging events as well as the degree of loss experienced by vulnerable elements in the past (Englhardt et al., 2019). Akbas et al., (2009) proposed specific physical vulnerability indicators introducing the concept of probabilistic damage functions and appropriate definition of relevant damage states, assessing temporal and spatial impact probability uncertainties. Vamvatsikos et al., (2010) in reviewing structural vulnerability assessment and existing

https://doi.org/10.5194/egusphere-2022-225
Preprint. Discussion started: 27 April 2022

methodologies under natural hazard, stressed a significant focus on the use of empirical data from past events and many efforts underway to provide powerful analytical tools to assess vulnerability at various scales (Apel et al., 2008). Notwithstanding, links between risk components remain the prerequisite for a consistent approach to steering a flood risk assessment. In the framework of flood risk analysis all components of the risk equation are spatially varying and linked, indicating the importance of the spatial patterns of risk assessment. An integrated approach based on spatially distributed information is required to better estimate risk components (Schanze J., 2006) . In this study we describe the development and the application of a quantitative method focusing on structural vulnerability assessment as a fundamental and dynamic component of flood risk analysis following the modified Source-Pathway-Receptor-Consequence (SPRC) conceptual model (Fleming, 2002). It relies a simple causal chain commonly adopted to understand the flood risk system and the link among its processes (Schanze J., 2006). The SPRC model consists of the hazard origin identification as to an event transmitted through a pathway to a receptor with possible negative effects for the receptor depending on their vulnerability and their exposure intensity considering events of different magnitudes (Hallegatte et al., 2013; Taramelli et al., 2015). The chain elements 'Source', 'Pathway' and 'Receptor' refer to the physical process, although the evaluation of the '(negative) Consequence' concerns economic and societal values. In terms of flood risk, 'Source' and 'Pathway' represent the flood hazard, the 'Pathway' can be described by the inland discharge or coastal overflow and inundation, 'Receptor' and '(negative) Consequence' state the exposure and the level of vulnerability. The article is organized as follows: after introducing the current methods to assess flood vulnerability and applications, Sect. 2 describes the case study. Section 3 addresses in detail the input data used and the analytic four steps of the SPRC approach to accurately assess the structural vulnerability. Section 4 depicts the structural vulnerability patterns characterized and classified in terms of their hazard to fluvial flooding based on data from the 2014 Seveso River flood event (Source and Pathway) and exposure, the developing of site-specific damage curves for the residential sector element at risk at meso (i.e., land use level) and microscale (i.e., building level) (Receptor and Consequence) and the damage mapping. Section 5 discusses the results of the study, especially regarding the potential of SPRC to improve the parameterization of the flood risk analysis' fundamentals at different scale of analysis and, finally, Sect. 6 summarizes the derived conclusions.

2 The Seveso river and the 2014 flood

The Lombardy region, Italy's economic engine, is particularly vulnerable to flood risk (Carrera et al., 2015). It is indeed the most flood-affected region in terms of financial damage, consequently influencing the national growth and stability. The northern part of the city of Milano (45° 28′, 09° 11′) is frequently flooded by the floodwaters of the Seveso River. 342 floods were reported in the last 140 years (i.e., 2.6 per year) (Becciu et al., 2018). On the 14th of July 2014 after a short and intense storm that dropped more than 60 mm of precipitation within 5 hours, the Seveso River overflowed in few sections along its course and flooded some densely populated areas in the provinces of Como, Monza-Brianza, and Milano. Notably, an area of about 3 km^2 in the northern part of the city of Milano was flooded, causing closure of streets and public transports and affecting thousands of inhabitants (http://floodlist.com/europe/seveso-river-floods-milan). The Seveso river overflowed at two sections

https://doi.org/10.5194/egusphere-2022-225
Preprint. Discussion started: 27 April 2022

at Niguarda (via Ca' Granda), flowing out of manholes and generating fountains of water and mud that completely inundated Viale Zara and the whole neighbourhood, frequently hit by similar events. The flood caused serious damage to cars, shops, basements and ground floors of many residential buildings. The Isola neighbourhood, near the historic city centre was also affected, and the area of Piazza Minniti was completely inundated. Throughout the northern part of the city, roads were paralyzed for many hours. Official loss data provided by the Lombardy Region based on Damage Report Form in the frame of the loss compensation by the State, reported a total damage of 27.2 million Euro. Private owners were the most impacted (64 %), followed by infrastructure (18 %), commercial activities (13 %), industrial sector (5 %) and environmental (0.4 %) (Fig. 1).

3 Material and Methods

In order to assess the structural vulnerability patterns and to understand the links among flood risk system processes we adopted a modified conceptual Source-Pathway- Receptor-Consequence (SPRC) Model.

The SPRC model considers the hazards as the flood water that propagates to the receptor resulting in potential consequences (Hallegatte et al., 2013; Taramelli et al., 2015) (Fig. 2):

- The ‘Source’ of a flood is the origin of the hazard, usually an extreme meteorological event (e.g., heavy rainfall) triggering floods.
- The ‘Pathway’ is the route that a hazard takes to get to the receptors. A pathway must exist for a hazard to be realized.
- The ‘Receptor’ refers to the entities that may be damaged by the hazard (e.g., people, property or the environment);
- The ‘Consequence’ is the impact such as economic, social or environmental that may result from a flood. It may be expressed quantitatively (e.g., monetary value), by category (e.g., high, medium, low) or descriptively.

In this section we address in detail the analytic four steps of the SPRC model to accurately assess the structural vulnerability (Fig. 3):

- Source estimation: we reassessed the "inundation map" replicating the flood characteristics providing the flood water depth extension for the study area affected zones.
- Pathway estimation: we defined inland attributes that can control and influence the event propagation.
- Receptor estimation: we considered the elements at risk to perform the exposure analysis and asset assessments. Thus, elements that are exposed to hazard have been categorized into vulnerability homogenous classes.
- Consequence estimation: we developed site-specific damage curves for the residential sector at meso (i.e., land use level) and microscale (i.e., building level) considering the 2014 flood event and three diverse flood scenarios assuming return periods of 10, 100 and 500 years (Hasanzadeh Nafari et al., 2013).

https://doi.org/10.5194/egusphere-2022-225
Preprint. Discussion started: 27 April 2022

3.1 Hazard scenarios definition: Source and Pathway estimation

3.1.1 Source Estimation

Polygons of the flooded area for this event were collected through the geoportal of the Regione Lombardia. The main data source is represented by surveys and observations from the affected municipalities. Flood related-hazard map of the 2014 flood event is attained by reconstructing the flood affected area and replicating the flood characteristics (i.e., depth of flood water) using the Floodwater Depth Estimation Tool version 2 (FwDET) (Cohen et al., 2019) implemented in Google Earth Engine. FwDET identifies the floodwater elevation for each cell within a flooded domain based on its nearest flood-boundary grid cell derived from the Digital Terrain Model (DTM), here at 5x5 m resolution.

3.1.2 Pathway Estimation

Morphological features and land use were also considered important factors in influencing hazard propagation. Specifically, sinks (SI) are low-lying areas in the urban landscape that can be considered areas where water pools in conditions of flooding and of an inefficient drainage system, endanger structures located within or near them (Dietrich and Perron, 2006; Dodov and Foufoula-Georgiou, 2006; Nardi et al., 2006; Taramelli and Reichenbach, 2008). These areas are defined including the DTM 5x5 m and the buildings' footprint layer into a sequential chain of GIS analysis tools. This model analyses the DTM with hydrology and selects buildings inside or adjacent to these low-lying areas. As the analysis was focused on residential sector damage, exposure information related only to built-up areas was extracted from Copernicus Urban Atlas 2018. These data are exploited to determine how flood risk could rise as a combination of environmental and climate changes effects (Taramelli et al., 2019). Imperviousness Degree map resampled at 5 m from Copernicus Land Monitoring Service is also used to identify most exposed residential buildings. Specifically, the normalized Imperviousness Surface Ratio (NISR) was introduced to obtain a proxy to identify buildings most exposed to hazard amplification due to soil sealing (S.L., as stated in the Land Cover/Land Use product nomenclature of the Copernicus Urban Atlas), Eq. (1).

$$NISR = \frac{\text{Imperviousness Degree}}{\text{Building Footprint}} \quad (1)$$

3.2 Exposure and structural vulnerability assessment: Receptor and Consequence estimation

At the building level, relevant structural factors (e.g., the building type, the period of construction, the material type, the maintenance state, and building height) are important for determining the damage due to flooding allowing specific building types classification. To evaluate the buildings potential degree of loss against flood hazards, the structural and non-structural building attributes were linked to the physical characteristics of the damaging flood events. Thus, the potential degree of loss has been obtained applying two different approaches:

- geographically-distributed and weight-base procedure at building level, the heuristic approach (Receptor Estimation);

https://doi.org/10.5194/egusphere-2022-225
Preprint. Discussion started: 27 April 2022

- site-specific and damage curves-based at both land use and building levels, the probabilistic approach (Consequence Estimation).

3.2.1 Receptors Estimation: Heuristic Approach

By overlapping hazard maps with the spatial distribution of the elements at risk, a corresponding hazard class is assigned to each building. This defines the magnitude of damaging flood assigned to each element at risk. Furthermore, at a residential building level relevant descriptive structural attributes are important for determining the damage due to flooding allowing specific building types classification (Figueiredo and Martina, 2016). The structural type combined with the construction materials determine the strength of the building. Age and maintenance are also indications for the current state of the building. Moreover, an estimation of elements-at-risk costs is fundamental to express losses in economic terms. The heuristic approach is based on a simple weights assignment procedure (Taramelli et al., 2015). By overlapping hazard maps with residential building map distribution , a corresponding hazard class is assigned to each building to obtain the element at risk class map (see Appendix A). A total score (Eq. 2) is calculated as the sum of single weights assigned to hazard (i.e., for water depth WD on the basis of the level in m of inland flooding raster maps, on sink SI map and on $NISR$ classes) (Table 1) and to each structural and non-structural factor (i.e., Construction Material Type MT, Period of Construction PT, Building Status BS, Building Height BH, Building Type BT) composing an element at risk. Weights are assigned from 1 = "no or very low response capacity" to 9 = "high response capacity" against flood (Table 2) (Corradi et al., 2015), and based on literature review (Taramelli et al., 2015).

$$\sum_i = (WD_i + SI_i + NISR_i) + (MT_i + PC_i + BS_i + BT_i + BH_i) \quad (2)$$

Hence, an Info-Table of residential buildings classified by total score is obtained. Residential buildings were classified in 5 vulnerability classes based on the obtained Info-Table from 'Very Low' to 'Very High' vulnerability (Table 3) and mapped considering the economic unit value in € m^{-2} based on National Real Estate Observatory (OMI) zone and relative market values quotation (€ m^{-2}) table obtained from OMI assigned to each residential building type (BT) on the basis of the building status (BS). Here the building economic unit value assumes solely the structure value excluding the content value. For buildings falling in most vulnerable classes (i.e., class 1 and 2, 'Very High' and 'High') a distinction was made between elements with and without basement assigning a weight of 0 to the building with basement and 1 to the building without basement (McBean et al., 1988; Crigg and Helweg, 1975).

3.2.2 Consequence Estimation: Probabilistic Approach

The analysis of the negative effects of different event types on exposed elements is necessary to assess the potential losses and the degree of damage of elements at risk. Fundamental to the vulnerability assessment is the concept of depth-damage functions defined as relations between floodwater depth and corresponding damage. Considering hazard scenarios, the depth-damage

https://doi.org/10.5194/egusphere-2022-225
Preprint. Discussion started: 27 April 2022

functions enable the estimation of expected direct losses, hinged on a spatial representation of flood process patterns and categorized elements at risk (Mazzorana et al., 2014). Although damage functions are generated for a specific building of a given type, they can be assumed as reliable predictors of damage for a group of buildings with similar structural/non-structural characteristics. The probabilistic approach is based on the use of damage model INSYDE (Dottori et al., 2016) implemented in R programming language. The model relies on an analysis of physical damages to buildings considering distinctive land use classes and building characteristic parameters to derive synthetic damage curves for residential buildings. Here, the INSYDE model was applied deterministically (i.e., without considering any source of uncertainty). To calculate the damage we combine the exposure and vulnerability data described above with the 2014 flood depth and considering three existing diverse flood depth scenarios assuming return periods of 10, 100 and 500 years derived from 1-D and 2-D hydraulic modelling designed by the Municipality of Milano in 2019 for the Governmental Territorial Plan and the Flood Risk Management Plan.

Modelled flood damage on residential buildings falling within the study by the following steps:

- Absolute damage was calculated obtaining the absolute damage function and the site-specific depth–damage curve for the residential sector;
- The annual average loss (AAL) and the exceedance probability (i.e., the probability that a certain damage value will be exceeded within a certain return period) for the residential sector were defined. This value is the expense that would occur in any given year if monetary damages from all hazard probabilities and magnitudes were spread out equally over time;
- Damage modelling and mapping at mesoscale analysis: new site-specific depth–damage functions are then developed for the residential sector at land use level. Potential maximum damage values for residential sector were attributed to each of the Urban Atlas 2018 land use class (i.e., other roads and associated land, industrial, commercial, public, military and private units, green urban areas, discontinuous medium urban fabric, discontinuous dense urban fabric, continuous urban fabric);
- Damage modelling and mapping at microscale analysis: new site-specific depth–damage functions are then developed for the residential sector at building level. Object-based water levels and damage data were integrated with information on building vulnerability considering most vulnerable buildings falling in class 1 and 2 (i.e., Very High and High vulnerability) as resulted from heuristic approach. Features and building characteristics parameters used as model input data are shown in the Appendix B. Therefore, we built depth–damage functions for two building category subsets based on structural and no structural characteristics frequency (see Fig.1C in the Appendix). In each category, a distinction was made between elements with and without basement. Here the functions are expressed by coupling the values of flood depth and damage factor (DF). The DF in the damage curves are intended to span from zero (no damage) to one (maximum damage), through absolute damage values normalization. Finally, absolute damage for each residential building was calculated by dividing total damage by building footprint (€ m^{-2}) and mapped to have spatially distributed information.

https://doi.org/10.5194/egusphere-2022-225
Preprint. Discussion started: 27 April 2022

4 Results

4.1 Hazard scenarios definition: Source and Pathway estimation

4.1.1 Source Estimation

Gridded estimates of flood depth were produced for the flood polygons of the event. A first quality check of the output denoted unrealistic values in urban areas, especially in the largest flood area in the municipality of Milano, with large portions of the city affected by flood depths of 2 m or larger (Fig. 4). This is in contrast with data reported by the media, referring to flood depths in the order of 30 cm. This is caused by the use of a flood polygon obtained by linking point observations and manual reports, rather than on a spatially continuous identification, such as those provided by aerial or satellite imagery. In addition, the large degree of urbanization in such area adds noise to the elevation data and consequently to the estimation of flood depths. Hence, in a following step we recomputed flood depths using a flood polygon where the shape of buildings (Open Street Maps, OSM) was first subtracted. In the resulting product, flood depths are mostly within the foreseen ranges, except for some areas with values above 5m along viale Fulvio Testi, Viale Zara and via Volturno. These are attributed to the construction of the line 5 of the underground train line of Milano, particularly to the stations named Ca' Granda, Istria, Marche, Zara and Isola, which took place in 2008-2010, at the same time of the survey campaign carried out to produce the DTM through Lidar measurements. After filling the holes of the underground stations in the DTM using neighbouring values, resulting flood depths are within realistic ranges, with mean depth of 19 cm and a 90th percentile of the flooded cells of 42 cm.

4.1.2 Pathway estimation

Sinks and at-risk buildings were identified and mapped (Fig. 5a). 1,246 buildings, the 81 % of the inundated residential buildings during the 2014 flood event, lie within or adjacent sink areas where water can potentially pool during a flood and amplify the hazard especially in case of inefficient drainage system. Based on Urban Atlas land use classes the 16.1% of the inundated built-up area was comprised of continuous urban fabric (where the 81% presents an average degree of S.L. > 80 %), the 82.8 % of discontinuous urban fabric (where the 49 % presents an average degree of S.L. between the 50 % and the 80 %) (Fig. 5b). Considering Copernicus Imperviousness Degree map resampled at 5m (Fig. 5c) and building footprint, the NISR has been calculated. Relating NISR to Urban Atlas land use classes, most exposed buildings to hazard amplification due to soil sealing fall into continuous (S.L. >80 %) and discontinuous (S.L. 50 %-80 %) dense urban fabric mostly located into areas with estimated water depth ranging between 0 and 0.20 m during the 2014 flood (Fig. 6).

https://doi.org/10.5194/egusphere-2022-225
Preprint. Discussion started: 27 April 2022

4.2 Exposure and structural vulnerability assessment: Receptor and Consequence estimation

4.2.1 Receptors Estimation: Heuristic Approach

Exposure analysis consisted in the recognition of potentially residential damaged assets (e.g., information on the location, number and type of elements at risk). 1540 residential building have been thereby classified and mapped according to structural and non-structural features including the attribution of economic values (Fig. 7).

We obtained an Info-table of residential buildings classified by hazard values derived by the weighting of hazard classes on the base of flood depth thresholds, sink map and NISR values and Total Weights derived by structural and non-structural features weighting. Total score varies from 9 to 34 showing distinct building response capacity against flooding. Low total score values stands for lower building response capacity or missing data. On the basis of the obtained total score, residential building structural vulnerability is mapped (Fig. 8a) distinguishing 5 classes (i.e., Very Low, Low, Moderate, High, Very High) and including the economic unit value based on their relative market values quotation (€ m^{-2}). 81 residential buildings fall in class 1 (0-17); 333 residential buildings fall in class 2 (18-20); 432 residential buildings fall in class 3 (21-23); 477 residential buildings fall in class 4 (24-27); 217 residential buildings fall in class 5 (28-39) (Fig. 8a). For 415 buildings falling in most vulnerable classes (i.e., class 1 and 2, 'Very High' and 'High' respectively) 185 buildings are characterised by the presence of a basement (Fig. 8d). Results show that most exposed buildings are mostly located in the southern highly urbanized part of the affected area, closer to the city centre, i.e., zone OMI C12 and C14. Calculating the average relative market values quotation for each vulnerability class we observed that the residential building falling in class 'Very High' showed the highest average value (i.e., 4148.2 € m^{-2}) (Table 4).

4.2.2 Consequence Estimation: Probabilistic Approach

Exposure analysis consisted in the recognition of potentially residential damaged assets (e.g., information on the location, number and type of elements at risk). 1540 residential building have been thereby classified and mapped according to structural and non-structural features including the attribution of economic values (Fig. 7).

To calculate the damage we combine the exposure and vulnerability data described above with the 2014 flood water depth assuming return periods of 500 , 100 and 10 years (Fig. 9).

Firstly, absolute damage has been calculated obtaining a damage function for the residential sector. Resulting total absolute damage to residential properties is equal to EUR 105.3 million, 100.8 million and 93 million assuming 500, 100 and 10 years of return period respectively and 62.4 million for 2014 flood. It is noteworthy that here the absolute damage modelled values for the considered return periods are always greater than the 2014 event values (Fig. 10a). As it can be seen by observing the depth–damage functions for the residential sector, the shape of the damage for 2014 flood is steeper until 0.2 m water depth than other functions. Nearly maximum damage occurs when water depths exceed 0.5 m. The three flood scenarios' function reach their maximum between 1.5 and 2 m (Fig. 10b). The obtained annual average loss (AAL) corresponds to EUR 18.3 million. Whilst the events with the lowest annual exceedance probability are associated with the highest total damages, showing

https://doi.org/10.5194/egusphere-2022-225
Preprint. Discussion started: 27 April 2022

that as probability decreases, damages increase (Fig. 10c). As third step, collected data for each inundated building in Milano were used for developing a site-specific mesoscale depth–damage curve for the residential sector (Fig. 11) and mapping (Fig. 12). At mesoscale absolute damage for each Urban Atlas 2018 land use class resulted higher for the 'Continuous urban fabric (S.L. : > 80 %)' class for all flood scenarios, and for the 2014 flood likewise (Fig. 11e). The function for the 'Continuous urban fabric (S.L. : > 80 %)' runs up to EUR 54.3 million considering the 500 years return period scenario (Fig. 11c). As can be seen, the shape of the damage for the 'Continuous urban fabric (S.L. : > 80 %) are similar for the 500 (Fig. 11c) and 100 (Fig. 11b) years return period scenarios. Whereas, for the 10 years return period scenario (Fig. 11a) and for the 2014 flood (Fig. 11d) the functions are much steeper in the first meter and in the first 0.2 m of water depth respectively. Therefore, the second highest maximum damages values are found for those residential buildings falling within 'Other roads and associated land' land use class with functions running up to maxima of EUR 27 million considering the 500 years return period scenario, reaching its maximum at about 2.5 m of water depth (Fig. 11c).

A more detailed, microscale analysis was then performed integrating object-based water levels and damage data with information on building vulnerability focusing on most vulnerable buildings falling in class 1 and 2 (i.e., Very High and High vulnerability) as resulted from heuristic approach. Specifically we built site-specific microscale depth–damage curve for two building category subsets based on structural and non-structural characteristics frequency (Appendix C) making a distinction between elements with and without basement: (1) BT='detached and semi-detached house'; MT='masonry'; BS='good'; NISR='0.05-0.12; BH=1-5 m; PC=1919-1966; (Fig. 13a); (2) BT='detached and semi-detached house'; MT='concrete'; BS='good'; NISR='0.05-0.12; BH=1-5 m; PC=1919-1966 (Fig. 13b). Considering the first subset the shape of the damage for the buildings with basement are not similar, notably the function for the 10 years return period scenario is much steeper in the first 4 m of water depth. The function for the 2014 flood is much steeper in the first 0.20 m of water depth, albeit its maximum value remains lower compared to the other flood scenarios. Considering the buildings without basement, the shape of the damage functions for the 10 and 100 years return period scenarios are quite similar, as the functions are much steeper in the first 0.5 m of water depth. However, difference with the 500 years return period becomes significant after the flooding depth exceeds 1 m. The function for the 2014 flood is much steeper in the first 0.30 m of water depth, although its maximum value remains lower compared to the other flood scenarios (Fig. 13a). Figure 13b shows the function for the 2014 flood of the building with basement much steeper in the first 0.30 m of water depth. Nearly maximum damage occurs when water depths exceed 0.3 m. As one can see, the shape of the damage curve for the 500 year return period differs significantly, as the function is less steep albeit it reaches higher maximum damage values at about 1.5 m. Looking at the buildings without basement, the shape of the damage functions for the 10 and 100 years return period scenarios are quite similar as for the 2014 and the 500 year return period scenario. The latter functions are much steeper in the first 0.20 m of water depth (Fig. 13b). Table 5 compares the flood depths for causing a DF equal to 0.1 for the two residential buildings subsets. In each subset, a distinction was made between elements with and without basement. Spatial distribution and variability are finally obtained by mapping absolute damage for each residential building calculated by dividing total damage by building footprint (€ m^{-2}) (Fig. 14).

https://doi.org/10.5194/egusphere-2022-225
Preprint. Discussion started: 27 April 2022

5 Discussion

In this study we described the development and the application of a quantitative method based on the causal chain of the SPRC focusing on structural vulnerability assessment as a fundamental and dynamic component of flood risk analysis in urban areas. We consider high vulnerability and exposure the outcome of skewed development process, such as those associate with the intensity of extreme and non-extreme climate and weather events, morphological features, buildings structural and non-structural characteristics and land use frequently associates to a rapid urbanization and suburbanization as for large metropolitan regions. Moreover, vulnerability can be seen as situation-specific and scale-dependent, interacting with a hazard event to generate risk. Therefore, capacity for risk prevention and reduction may be understood as a series of elements, measures, and tools directed toward intervention in hazards and vulnerabilities with the objective of reducing existing or controlling future possible risks (Cardona, 2013) at diverse scale of analysis. Empirical measures of the 2014 flood event allowed a valid characterization of the hazard system and the intrinsic, underlying relationships and interdependencies required in the structural vulnerability assessment framework.

5.1 Hazard scenarios definition: Source and Pathway estimation

Starting with source estimation, we reassessed the 2014 flood characteristics in a densely urbanized area of Milano obtaining flood depths values within the foreseen ranges, a worthwhile data for the study of highly flood-prone residential buildings. This requires knowledge about how the source interactions with the natural and non-natural environment lead to the amplification or the reduction of hazards. The methodology used produces accurate estimates of the flood characteristics, with mean error in flood depths estimation in the range 0.2-0.3 m (Cohen et al., 2019). Yet, it enables realistic representation of the flood extent, with robust performance. Furthermore, it is scalable to larger domains and particularly suitable for coupling with satellite-derived flood extents. In contrast, applications in urban areas are especially challenging, and may need manual fine-tuning to overcome a range of issues coming from the flood characteristics, elevation data, building size and underground structures, among others. Indeed, the environment offers resources for human development at the same time as it represents exposure to intrinsic and fluctuating hazardous conditions (Lal et al., 2012). Between the 2012 and the 2018 in the Milano metropolitan region the 58 % of land use changes concerns the urban expansion uptake of agricultural areas (European Environment Agency, 2018). Thus, we estimated the pathway analysing land use focusing on residential built-up areas identifying low-lying and impervious surfaces (Fig. 5c). In this zone low-lying areas are already affected by periodic flooding after heavy rainfall and greater urbanization and sprawl could exacerbate this problem. Thus, buildings adjacent or close to these areas are considered at greater risk of being flooded (Fig. 5a). As is evident from the results NISR higher values fall within low-lying area. However, these no longer coincide with higher values of water depth recorded for the 2014 flood event (Fig. 6). Therefore, in areas that are already developed, sink map and NISR class can be used to prioritize areas for better risk mitigation planning purposes.

https://doi.org/10.5194/egusphere-2022-225
Preprint. Discussion started: 27 April 2022

5.2 Exposure and structural vulnerability assessment: Receptor and Consequence estimation

By assessing the exposure we defined the receptors and consequently how vulnerability varies spatially. The heuristic approach ingests residential building exposure categories, source and pathway estimation outputs, meeting the need to achieve a fast, though approximate, vulnerability estimation at building level (Fig. 8). The majority of the residential buildings fall in classes 'Low' and 'Moderate' (Fig. 8). Moreover, residential buildings falling in class 'High' and 'Very High' are mostly houses built of masonry between the 1919 and the 1970 in a good state of maintenance, of which most with a basement, and the highest average economic unit value in € m^{-2} (Table 4). These buildings are also located where NISR is higher demonstrating that is a valid support for quantifying buildings most exposed to hazard amplification especially in dense urbanized areas (Fig. 5c). The method resulted to be valuable as a preliminary assessment of the potential weaknesses in the structural building system to be used in the consequence estimation. Consequence estimation relates to the probabilistic phase of the structural vulnerability based on different scales of model application to obtain the AAL, which is a rough measure of the absolute "riskiness" of a set of exposures and refers to the long-term expected losses per year (i.e., averaged over many years), and the site-specific depth–damage curves (such as meso and microscale curves). Thereby exposed assets as a function of water level were then translated into absolute damage. At mesoscale the 'Continuous urban fabric' Urban Atlas 2018 land-use class with the occurrence of at least 80 % of soil sealing shows higher absolute damage values. Residential buildings falling in the 'Roads and associated land' class likewise show great absolute damage values. Roads accounted for the increase in impervious cover giving a significant impact on natural water systems (Figs. 11 and 12). Whereas less values of absolute damage are measured for those building located close to 'Green urban areas' is noteworthy (Figs. 11 and 12). At microscale we considered two subsets of buildings falling in most vulnerable classes (i.e., class 1 and 2, 'Very High' and 'High') as resulted from heuristic approach building obtaining site-specific depth-damage curves. Observing Table 5 that compares the flood depths needed for causing a DF equal to 0.1 for the different building types, similar values were found for all buildings 'with basement' for the three flood scenarios, and they increased for buildings 'without basement' structures. A possible explanation for this might be due to a larger residence time of water and to the 'filling effect' occurring in basements. It is important to underline that a DF equal to 0.1 for the 2014 is reached at lower values of flood depths for both the subsets, demonstrating that even events with moderate magnitude in terms of flood depth in a complex urbanized area may cause more damage than it would expect.

In general from the findings some key observations emerge:

- At mesoscale the idea that impervious surfaces amplify flood hazards and cause more relevant direct and tangible damage to structures is reinforced. One consequence of increasing impervious cover in urban areas is that conventional urban stormwater systems with underground piping can be overwhelmed when run-off exceeds the capacity of the system and cause surface flooding as for the city of Milano;
- Structural vulnerability measurement and patterns understanding is improved: we derived where vulnerability occurred and how vulnerability was distributed at local scale;

https://doi.org/10.5194/egusphere-2022-225
Preprint. Discussion started: 27 April 2022

- New insights were given for the development of site-specific local residential depth–damage curves for a more comprehensive description of residential buildings damage processes and parameterization across two spatial scale of analysis. Flood damage modelling on the building level is important to optimize investments for the implementation of flood risk management concepts in urban areas.

However, some limitations can be noted. In Italy the current national and regional databases are often of insufficient quality to support a comparative assessment between past damage events data to those findings obtained by depth-damage functions reported in the literature. Moreover one of the three main elements to be correlated among hazard, vulnerability, and damage is often missing or too hazy to make an appropriate comparison (Molinari et al., 2014). As for the latter point, available products and services of the European Copernicus Earth Observation program can be a valid support to bridge this gap. Specifically, Copernicus Land Monitoring Service products here provided valuable data to extract environmental features and physical exposure information due to the synoptic overview that enables to capture the totality of the landscape elements that influence the vulnerability patterns.

6 Conclusion

The goal of this study was to analyse structural vulnerability patterns to enhance the parameterisation of the flood damage assessment model for the residential sector. Data associated to past damaging floods have been elaborated for the purpose of evaluating the vulnerability of a portion of the urbanized area of Milano in relation to the flood intensity. Results provide a basis to obtain residential building-scale flood loss estimation and site-specific damage mapping. At building level structural vulnerability classes stood strictly driven by the structural type combined with the construction materials, building age and basement presence. On the basis of the 5 structural vulnerability classes the economic unit value based on their relative market values quotation describes that most exposed buildings, mostly located in the southern highly urbanized part of the affected area, are the one with the highest average market value. Besides buildings attributes, findings indicate that also extrinsic parameters describing the geographical context, such as morphological features and land use, indirectly affected vulnerability spatial distribution highly influencing hazard propagation. This aspect of the research suggested that our results provide evidence for an integrated flood risk management that should consider the entire flood risk system and the interaction among each process. Once SPRC is determined, such a model can be adopted to:

- Characterizing vulnerability patterns of urban flood damaging event within the bounds of this study at suitable spatial resolution;
- Evaluating impacts at building and landscape scale as a consequence of human interventions on river basins (e.g., river training, loss of flood plains and the retention capacity, the increase of impervious surfaces, large changes of land cover and intensified land use in particular for the development of settlements);

https://doi.org/10.5194/egusphere-2022-225
Preprint. Discussion started: 27 April 2022

- Significantly supporting decision-making processes based on cost-efficiency to prioritize effective interventions for flood risk reduction and mitigation boosting the change from the paradigm of flood protection to the paradigm of flood risk management (Klijn et al., 2008; Thomas and Knüppe, 2016);
- Minimizing the flood risk through changing any of the four elements of the conceptual model.

Appendix A

Hazard classes for flood depth on the basis of the level in m of inland flooding raster maps were assigned to residential buildings using the ZONAL STAT tool considering the maximum value (i.e., the largest value of all cells in the value raster that belong to the same zone as the output cell) on the basis of flood depth thresholds used for the hazard classification in the definition of Lombardy Region Territorial Coordination Plan (Fig. A1).

Appendix B

We assumed default values for missing variables (Table B1 and B2).

Appendix C

Structural and no structural building characteristics frequency distribution has been calculated according to vulnerability classes obtained from the heuristic approach (Fig. C1).

Author contribution

AT supervised and acquired the financial support for the project leading to this publication. EV and MR developed the methodology. MR, LA, SG and IG analysed data and performed the models. MR and IG prepared the manuscript draft with contributions from all co-authors. AT, EV, MR, LA, IG reviewed and edited the manuscript.

Acknowledgements

Financial Support

This research has been supported by EFLIP, a project funded by Fondazione CARIPLO (grant nos.2017-0735).

https://doi.org/10.5194/egusphere-2022-225
Preprint. Discussion started: 27 April 2022

References

Akbas, S., Blahut, J., and Sterlacchini, S.: Critical assessment of existing physical vulnerability estimation approaches for debris flows, Landslide Process. from Geomorphol. Mapp. to Dyn. Model., 229–233, 2009.

Apel, H., Merz, B., and Thieken, A. H.: Quantification of uncertainties in flood risk assessments, Int. J. River Basin Manag., 6, 149–162, https://doi.org/10.1080/15715124.2008.9635344, 2008.

Becciu, G., Ghia, M., and Mambretti, S.: A century of works on river seveso: From unregulated development to basin reclamation, Int. J. Environ. Impacts Manag. Mitig. Recover., 1, 461–472, https://doi.org/10.2495/ei-v1-n4-461-472, 2018.

Bouwer, L. M., Bubeck, P., and Aerts, J. C. J. H.: Changes in future flood risk due to climate and development in a Dutch polder area, Glob. Environ. Chang., 20, 463–471, https://doi.org/10.1016/j.gloenvcha.2010.04.002, 2010.

Cammerer, H. and Thieken, A. H.: Historical development and future outlook of the flood damage potential of residential areas in the Alpine Lech Valley (Austria) between 1971 and 2030, Reg. Environ. Chang., 13, 999–1012, https://doi.org/10.1007/s10113-013-0407-9, 2013.

Cammerer, H., Thieken, A. H., and Verburg, P. H.: Spatio-temporal dynamics in the flood exposure due to land use changes in the Alpine Lech Valley in Tyrol (Austria), Nat. Hazards, 68, 1243–1270, https://doi.org/10.1007/s11069-012-0280-8, 2013.

Cardona, O. D.: The need for rethinking the concepts of vulnerability and risk from a holistic perspective: A necessary review and criticism for effective risk management, Mapp. Vulnerability Disasters, Dev. People, 37–51, https://doi.org/10.4324/9781849771924, 2013.

Carrera, L., Climatici, C., Eni, F.-F., Mattei, E., Standardi, G., Cmcc, F., Elco, F., Koks, E., Feyen, A. L., Aerts, J., Bosello, F., and Amsterdam, F.: Economics of flood risk in Italy under current and future climate, 2015.

Cohen, S., Raney, A., Munasinghe, D., Loftis, J. D., Molthan, A., Bell, J., Rogers, L., Galantowicz, J., Brakenridge, G. R., Kettner, A. J., Huang, Y.-F., and Tsang, Y.-P.: The Floodwater Depth Estimation Tool (FwDET v2.0) for improved remote sensing analysis of coastal flooding, Nat. Hazards Earth Syst. Sci., 19, 2053–2065, https://doi.org/10.5194/nhess-19-2053-2019, 2019.

Corradi, J., Salvucci, G., and Vitale, V.: Analisi della vulnerabilità sismica dell ' edificato italiano : tra demografia e " domografia " una proposta metodologica innovativa, 1–22, 2015.

Crigg, N. S. and Helweg, O. J.: State-of-the-Art of Estimating Flood Damage in Urban Areas, Am. Water Resour. Assoc., 11,

379–390, 1975.

Cutter, S. L. and Finch, C.: Temporal and spatial changes in social vulnerability to natural hazards, Proc. Natl. Acad. Sci., 105, 2301 LP – 2306, https://doi.org/10.1073/pnas.0710375105, 2008.

Dietrich, W. E. and Perron, J. T.: The search for a topographic signature of life., Nature, 439, 411–418, https://doi.org/10.1038/nature04452, 2006.

Dodov, B. A. and Foufoula-Georgiou, E.: Floodplain morphometry extraction from a high-resolution digital elevation model: a simple algorithm for regional analysis studies, IEEE Geosci. Remote Sens. Lett., 3, 410–413, https://doi.org/10.1109/LGRS.2006.874161, 2006.

Dottori, F., Figueiredo, R., Martina, M. L. V., Molinari, D., and Scorzini, A. R.: INSYDE: A synthetic, probabilistic flood damage model based on explicit cost analysis, Nat. Hazards Earth Syst. Sci., 16, 2577–2591, https://doi.org/10.5194/nhess-16-2577-2016, 2016.

Elmer, F., Thieken, A. H., Pech, I., and Kreibich, H.: Influence of flood frequency on residential building losses, Nat. Hazards Earth Syst. Sci., 10, 2145–2159, https://doi.org/10.5194/nhess-10-2145-2010, 2010.

Englhardt, J., de Moel, H., Huyck, C. K., de Ruiter, M. C., Aerts, J. C. J. H., and Ward, P. J.: Enhancement of large-scale flood risk assessments using building-material-based vulnerability curves for an object-based approach in urban and rural areas, Nat. Hazards Earth Syst. Sci., 19, 1703–1722, https://doi.org/10.5194/nhess-19-1703-2019, 2019.

European Environment Agency: Mapping Guide v6.1 European for a European Urban Atlas, 1–228, 2018.

Faella, C. and Nigro, E.: Dynamic impact of the debris flows on the constructions during the hydrogeological disaster in Campania -1998: Failure mechanical models and evaluation of the impact velocity, 2003.

Figueiredo, R. and Martina, M.: Using open building data in the development of exposure data sets for catastrophe risk modelling, Nat. Hazards Earth Syst. Sci., 16, 417–429, https://doi.org/10.5194/nhess-16-417-2016, 2016.

Fleming, G.: Learning to live with rivers—the ICE's report to government, Proc. Inst. Civ. Eng. - Civ. Eng., 150, 15–21, https://doi.org/10.1680/cien.2002.150.5.15, 2002.

Hallegatte, S., Green, C., Nicholls, R. J., and Corfee-Morlot, J.: Future flood losses in major coastal cities, Nat. Clim. Chang., 3, 802–806, https://doi.org/10.1038/nclimate1979, 2013.

https://doi.org/10.5194/egusphere-2022-225
Preprint. Discussion started: 27 April 2022

Hasanzadeh Nafari, R., Ballio, F., Menoni, S., and Molinari, D.: Flood damage assessment with the help of HEC-FIA model Faculty of Civil and Environmental Engineering Master of Science in Civil Engineering for Risk Mitigation (CERM) Supervisors, https://doi.org/10.13140/RG.2.1.4779.8480, 2013.

Hufschmidt, G., Crozier, M., and Glade, T.: Natural Hazards and Earth System Sciences Evolution of natural risk: research framework and perspectives, Nat. Hazards Earth Syst. Sci., 5, 375–387, 2005.

Klijn, F., Samuels, P., and Van Os, A.: Towards flood risk management in the eu: State of affairs with examples from various european countries, Int. J. River Basin Manag., 6, 307–321, https://doi.org/10.1080/15715124.2008.9635358, 2008.

Lal, P. N., Mitchell, T., Aldunce, P., Auld, H., Mechler, R., Miyan, A., Romano, L. E., Zakaria, S., Dlugolecki, A., Masumoto, T., Ash, N., Hochrainer, S., Hodgson, R., Islam, T. U., Mc Cormick, S., Neri, C., Pulwarty, R., Rahman, A., Ramalingam, B., Sudmeier-Reiux, K., Tompkins, E., Twigg, J., and Wilby, R.: National systems for managing the risks from climate extremes and disasters, 339–392 pp., https://doi.org/10.1017/CBO9781139177245.009, 2012.

Mazzorana, B., Simoni, S., Scherer, C., Gems, B., Fuchs, S., and Keiler, M.: A physical approach on flood risk vulnerability of buildings, Hydrol. Earth Syst. Sci., 11, https://doi.org/10.5194/hessd-11-1411-2014, 2014.

McBean, E. A., Gorrie, J., Fortin, M., Ding, J., and Monlton, R.: Adjustment Factors for Flood Damage Curves, J. Water Resour. Plan. Manag., 114, 635–646, https://doi.org/10.1061/(asce)0733-9496(1988)114:6(635), 1988.

Merz, B., Kreibich, H., Schwarze, R., and Thieken, A.: Review article "assessment of economic flood damage," Nat. Hazards Earth Syst. Sci., 10, 1697–1724, https://doi.org/10.5194/nhess-10-1697-2010, 2010.

Meyer, V., Becker, N., Markantonis, V., Schwarze, R., Van Den Bergh, J. C. J. M., Bouwer, L. M., Bubeck, P., Ciavola, P., Genovese, E., Green, C., Hallegatte, S., Kreibich, H., Lequeux, Q., Logar, I., Papyrakis, E., Pfurtscheller, C., Poussin, J., Przyluski, V., Thieken, A. H., and Viavattene, C.: Review article: Assessing the costs of natural hazards-state of the art and knowledge gaps, Nat. Hazards Earth Syst. Sci., 13, 1351–1373, https://doi.org/10.5194/nhess-13-1351-2013, 2013.

Molinari, D., Menoni, S., Aronica, G. T., Ballio, F., Berni, N., Pandolfo, C., Stelluti, M., and Minucci, G.: Ex post damage assessment: An Italian experience, Nat. Hazards Earth Syst. Sci., 14, 901–916, https://doi.org/10.5194/nhess-14-901-2014, 2014.

Morelli, A., Taramelli, A., Bozzeda, F., Valentini, E., Colangelo, M. A., and Cueto, Y. R.: The disaster resilience assessment of coastal areas: A method for improving the stakeholders' participation, Ocean Coast. Manag., 214, https://doi.org/10.1016/j.ocecoaman.2021.105867, 2021.

https://doi.org/10.5194/egusphere-2022-225
Preprint. Discussion started: 27 April 2022

Nardi, F., Vivoni, E. R., and Grimaldi, S.: Investigating a floodplain scaling relation using a hydrogeomorphic delineation method, Water Resour. Res., 42, 1–15, https://doi.org/10.1029/2005WR004155, 2006.

Nasiri, H., Mohd Yusof, M. J., and Mohammad Ali, T. A.: An overview to flood vulnerability assessment methods, Sustain. Water Resour. Manag., 2, 331–336, https://doi.org/10.1007/s40899-016-0051-x, 2016.

Roberts, N. J., Nadim, F., and Kalsnes, B.: Quantification of vulnerability to natural hazards, Georisk Assess. Manag. Risk Eng. Syst. Geohazards, 3, 164–173, https://doi.org/10.1080/17499510902788850, 2009.

Schanze J.: FLOOD RISK MANAGEMENT – A BASIC FRAMEWORK, in: Flood Risk Management: Hazards, Vulnerability and Mitigation Measures, edited by: Schanze, J., Zeman, E., and Marsalek, J., Springer Netherlands, Dordrecht, 1–20, https://doi.org/10.1007/978-1-4020-4598-1_1, 2006.

Taramelli, A. and Reichenbach, P.: Comparison of Srtm Elevation Data With Cartographically Derived DEMs in Italy, Rev. Geogr. Acad., 2, 41–52, 2008.

Taramelli, A., Valentini, E., and Sterlacchini, S.: A GIS-based approach for hurricane hazard and vulnerability assessment in the Cayman Islands, Ocean Coast. Manag., 108, 116–130, https://doi.org/10.1016/j.ocecoaman.2014.07.021, 2015.

Taramelli, A., Manzo, C., Valentini, E., and Cornacchia, L.: Coastal Subsidence: Causes, Mapping, and Monitoring, in: Natural Hazards: Earthquakes, Volcanoes, and Landslides, edited by: Ramesh Singh, D. B., CRC Press, 253–290, 2018.

Taramelli, A., Lissoni, M., Piedelobo, L., Schiavon, E., Valentini, E., Nguyen Xuan, A., and González-Aguilera, D.: Monitoring Green Infrastructure for Natural Water Retention Using Copernicus Global Land Products, Remote Sens., 11, https://doi.org/10.3390/rs11131583, 2019.

Thieken, A. H., Olschewski, A., Kreibich, H., Kobsch, S., and Merz, B.: Development and evaluation of FLEMOps - A new Flood Loss Estimation MOdel for the private sector, WIT Trans. Ecol. Environ., 118, 315–324, https://doi.org/10.2495/FRIAR080301, 2008.

Thomas, F. and Knüppe, K.: From Flood Protection to Flood Risk Management: Insights from the Rhine River in North Rhine-Westphalia, Germany, Water Resour. Manag., 30, 2785–2800, https://doi.org/10.1007/s11269-016-1323-9, 2016.

UN Secretary-General: Report of the open-ended intergovernmental expert working group on indicators and terminology relating to disaster risk reduction, 21184, 1–41, 2016.

UNISDR: Words into Action Guidelines: National Disaster Risk Assessment (Governance System, Methodologies, and Use

https://doi.org/10.5194/egusphere-2022-225
Preprint. Discussion started: 27 April 2022

of Results), UN Off. Disaster Risk Reduct., 303, 2017.

Vamvatsikos, D., Kouris, L. A., Panagopoulos, G., Kappos, A. J., Nigro, E., Rossetto, T., Lloyd, T. O., and Stathopoulos, T.: Structural vulnerability assessment under natural hazards: A review, COST ACTION C26 Urban Habitat Constr. under Catastrophic Events - Proc. Final Conf., 711–723, 2010.

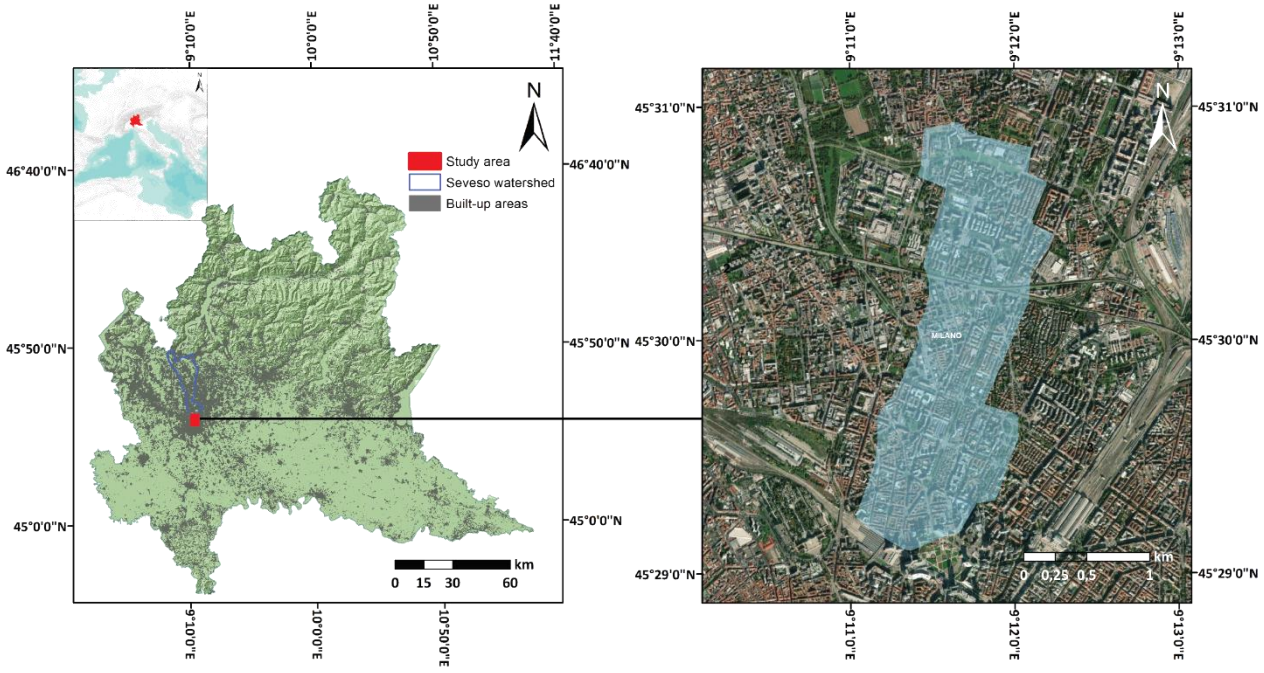

Figure 1: Investigation area and survey of inundated area of 2014 Seveso flood in Milano. Base map and DTM from © Regione Lombardia 2022. Built-up areas shapefile is from © OpenStreetMap contributors 2022. Distributed under the Open Data Commons Open Database License (ODbL) v1.0. Satellite image is from © Google Earth 2022.

https://doi.org/10.5194/egusphere-2022-225
Preprint. Discussion started: 27 April 2022

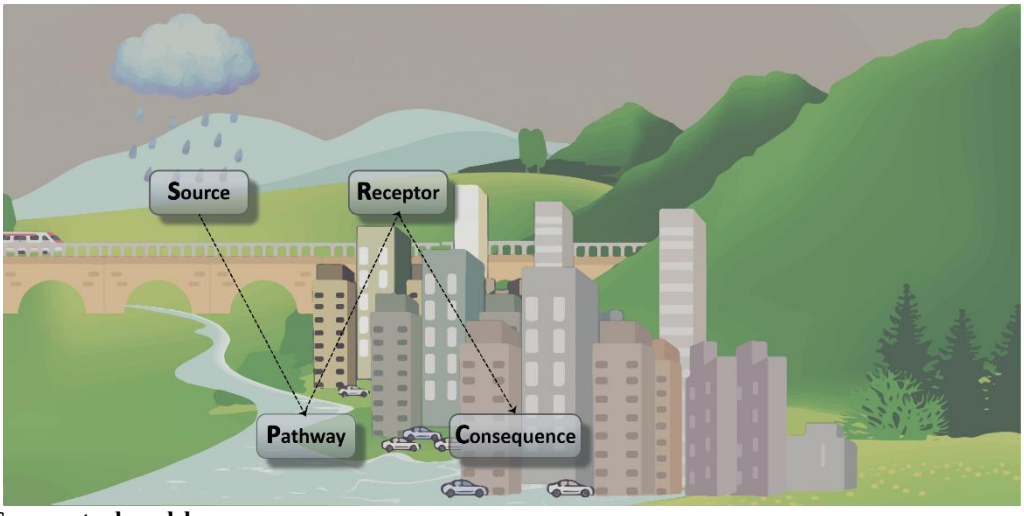

Figure 2: SPRC conceptual model.

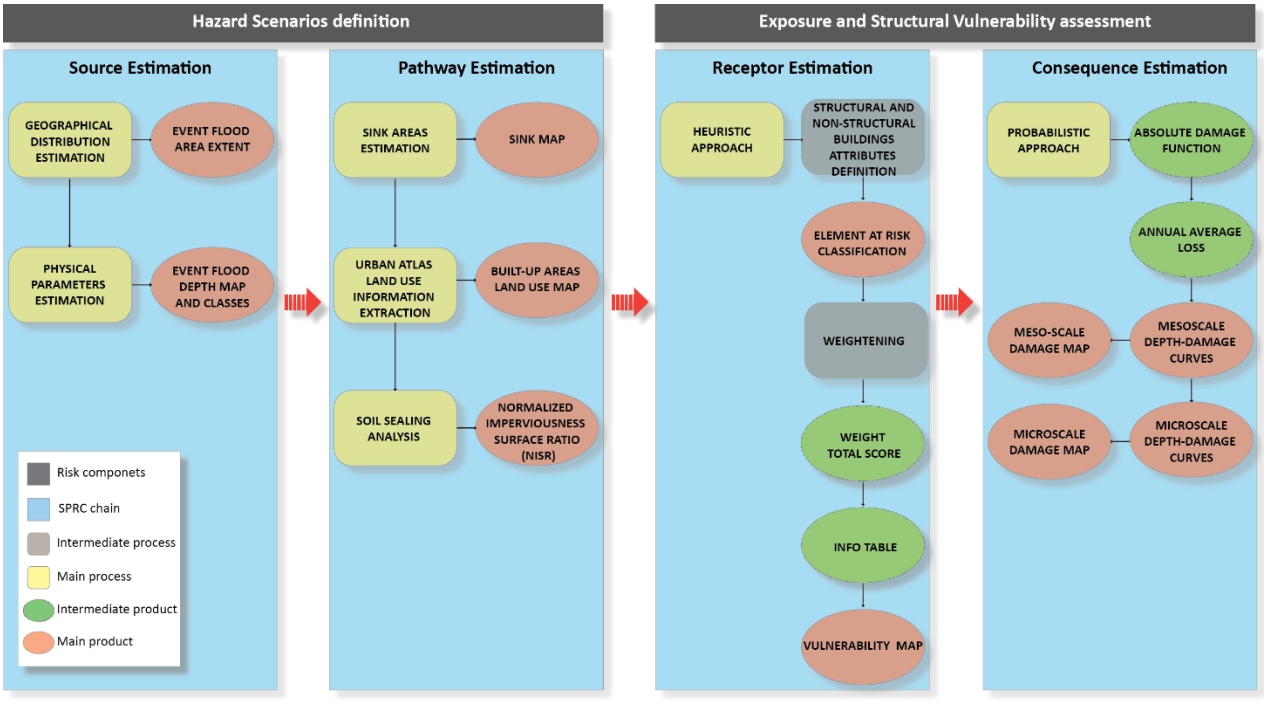

Figure 3: Structural vulnerability assessment procedure overview using a modified SPRC model.

https://doi.org/10.5194/egusphere-2022-225
Preprint. Discussion started: 27 April 2022

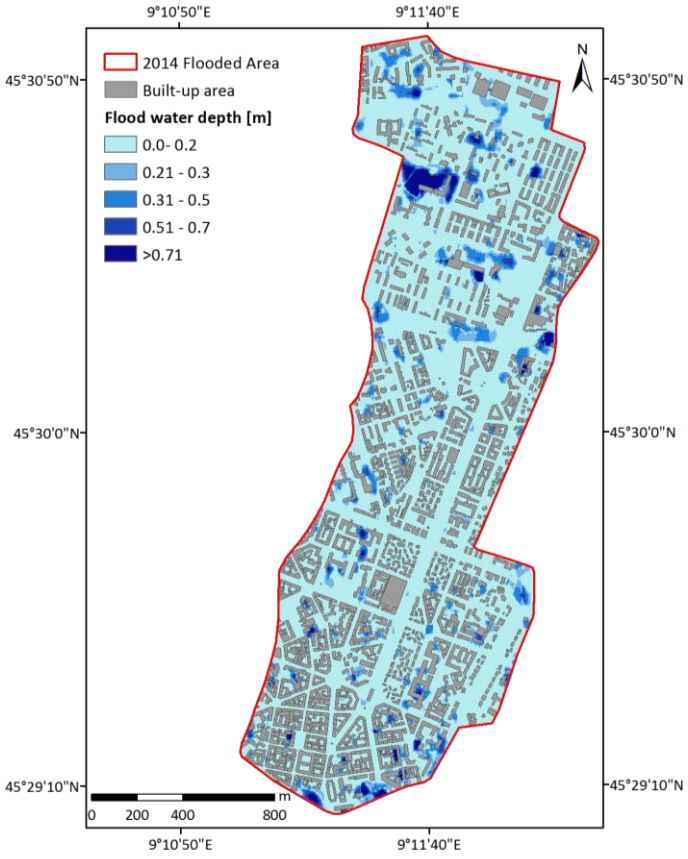

Figure 4: Estimated flood depths for the flooded polygon in Milano. Built-up areas shapefile from © OpenStreetMap contributors 2022. Distributed under the Open Data Commons Open Database License (ODbL) v1.0. Base map is from © Regione Lombardia 2022.

https://doi.org/10.5194/egusphere-2022-225
Preprint. Discussion started: 27 April 2022

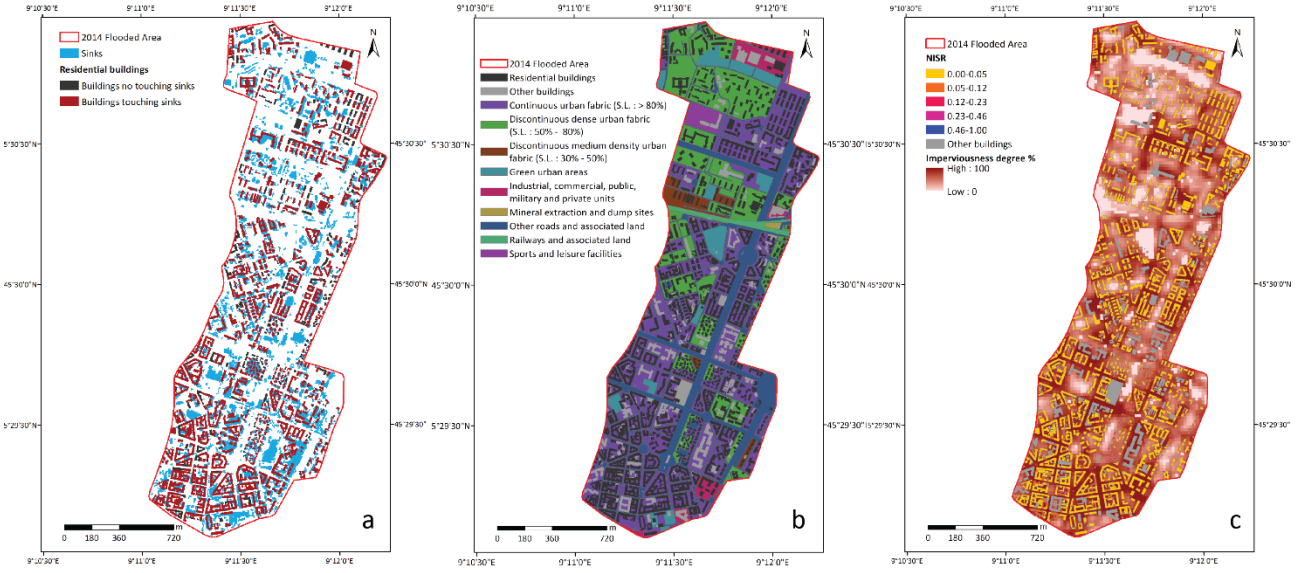

Figure 5: (a) Sinks distribution map (touching sinks in red; non touching sinks in grey); (b) Urban Atlas 2018 map (residential buildings in black; other buildings in grey (c) Copernicus Imperviousness Degree map resampled at 5m and NIRS distribution for residential building. Built-up areas shapefile is from © OpenStreetMap contributors 2022. Distributed under the Open Data Commons Open Database License (ODbL) v1.0. Base maps in (b) and (c) are from © European Union, Copernicus Land Monitoring Service 2022, European Environment Agency (EEA).

https://doi.org/10.5194/egusphere-2022-225
Preprint. Discussion started: 27 April 2022

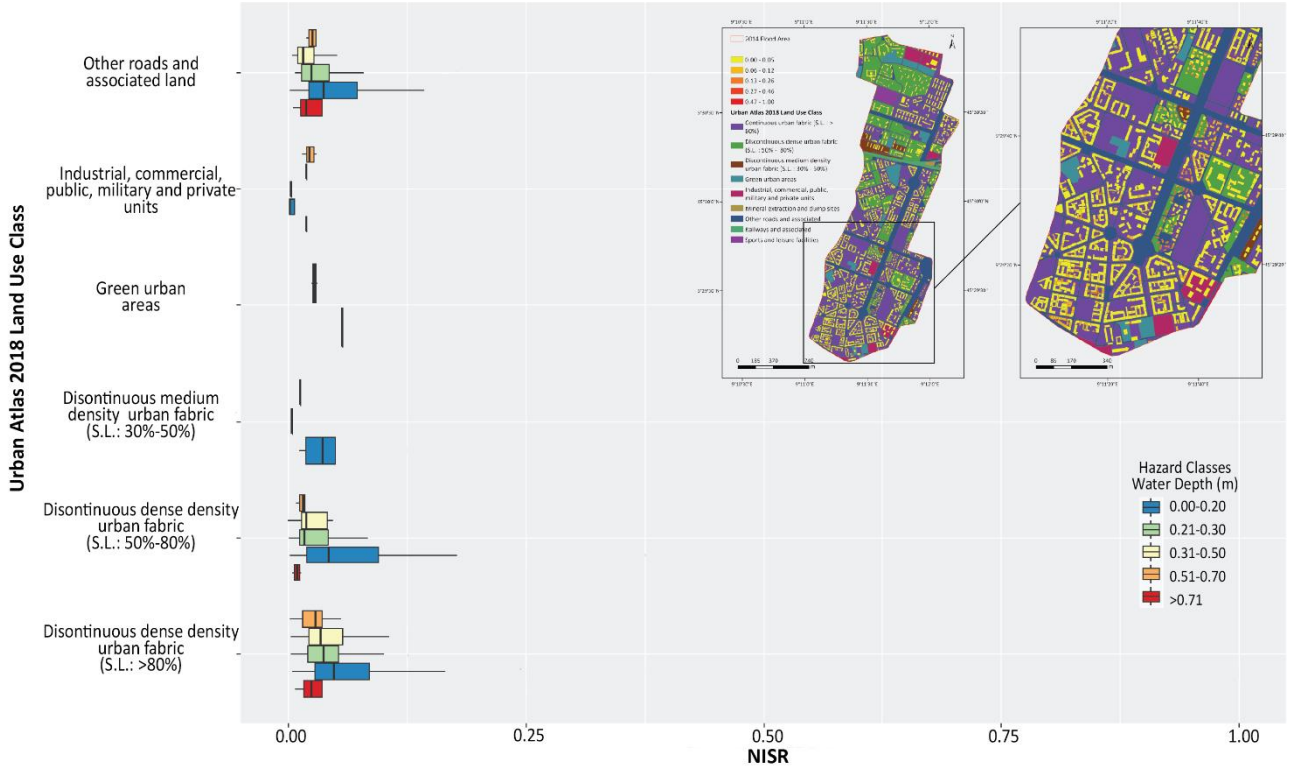

Figure 6: Boxplots and maps of NIRS distribution for residential building according to Urban Atlas 2018 land use classes and water depth hazard classes. Built-up areas shapefile is from © OpenStreetMap contributors 2022. Distributed under the Open Data Commons Open Database License (ODbL) v1.0. Base map is from © European Union, Copernicus Land Monitoring Service 2022, European Environment Agency (EEA).

https://doi.org/10.5194/egusphere-2022-225
Preprint. Discussion started: 27 April 2022

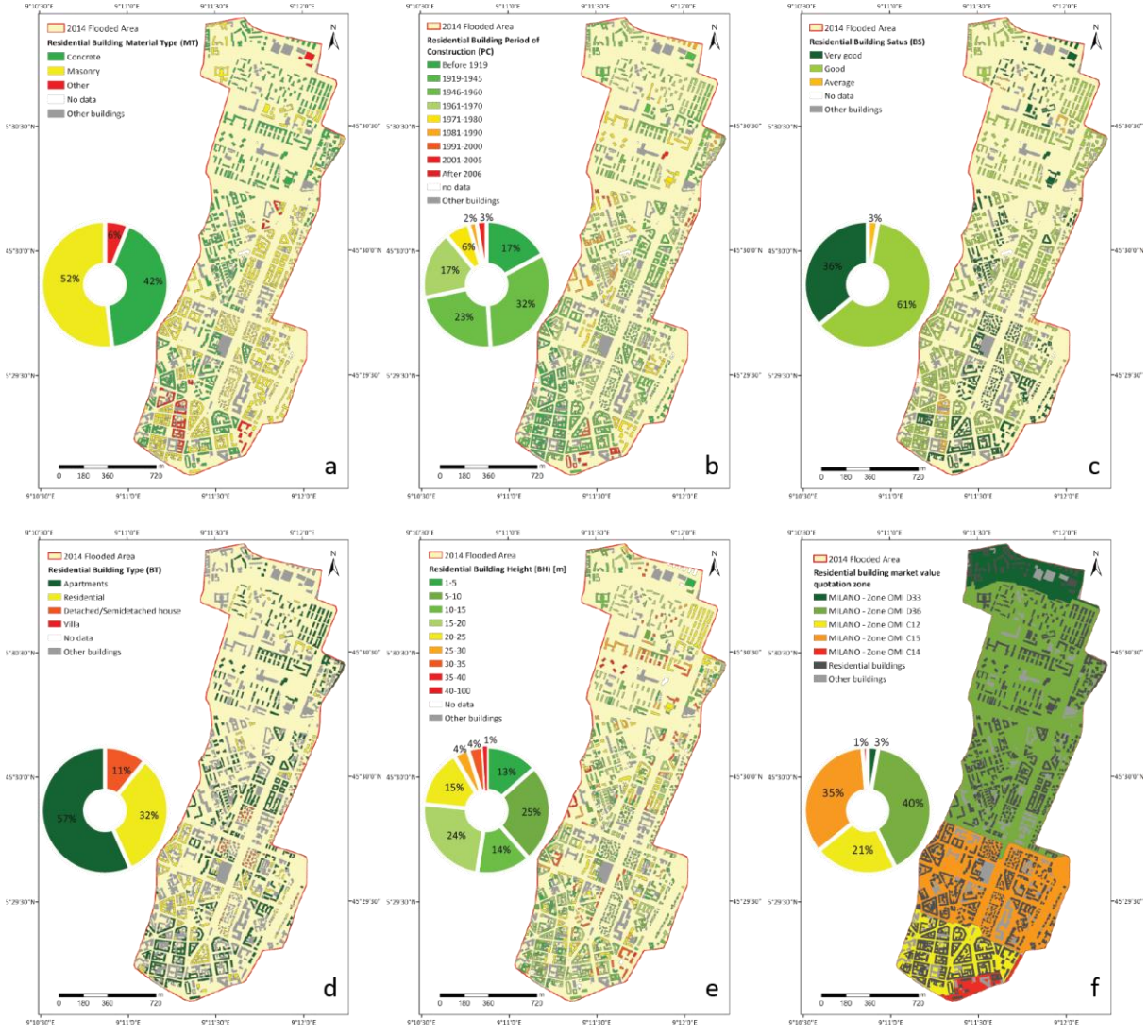

Figure 7: Residential Buildings: (a) material type map (MT); (b) period of construction map (PC); (c) building status (BS) map; (d) building type map (BT); (e) building height map (BH); (f) OMI zone map and relative market values quotation (€/m^2). Pie charts represent the percentages of residential buildings distribution according to structural and non-structural feature. Built-up areas shapefile is from © OpenStreetMap contributors 2022. Distributed under the Open Data Commons Open Database License (ODbL) v1.0. Base map in (f) is from © Geopoi, Map Data 2022.

https://doi.org/10.5194/egusphere-2022-225
Preprint. Discussion started: 27 April 2022

https://doi.org/10.5194/egusphere-2022-225
Preprint. Discussion started: 27 April 2022

Figure 8: (a) Residential buildings maps classified by vulnerability class and frequency; (b) most vulnerable residential buildings with and without basement map; examples of residential buildings falling in class High and Very High (c) without basement and (d) with basement respectively and (e) their location. Built-up areas shapefile is from © OpenStreetMap contributors 2022. Distributed under the Open Data Commons Open Database License (ODbL) v1.0. Building pictures are from © Google Maps 2022.

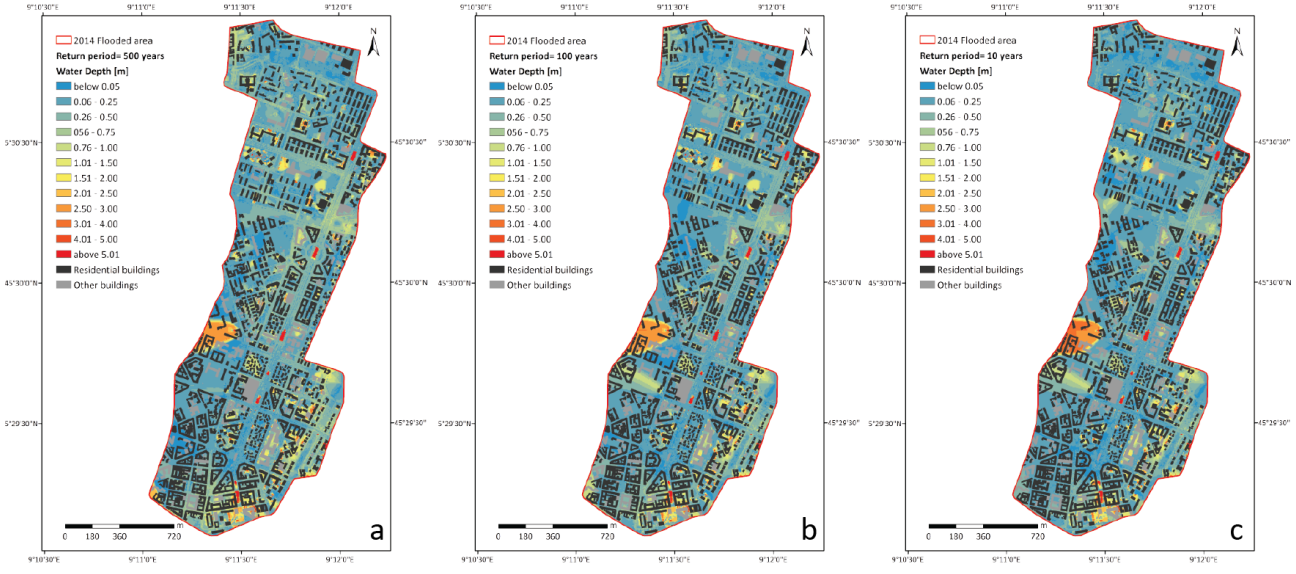

Figure 9: Estimated water depth and probability of flooding assuming (a) 500, (b) 100 and (c) 10 years of return period scenarios derived from 1-D and 2-D hydraulic modelling designed by the Municipality of Milano in 2019 for the Governmental Territorial Plan and the Flood Risk Management from © Regione Lombardia 2022. Built-up areas shapefile is from © OpenStreetMap contributors 2022. Distributed under the Open Data Commons Open Database License (ODbL) v1.0.

https://doi.org/10.5194/egusphere-2022-225
Preprint. Discussion started: 27 April 2022

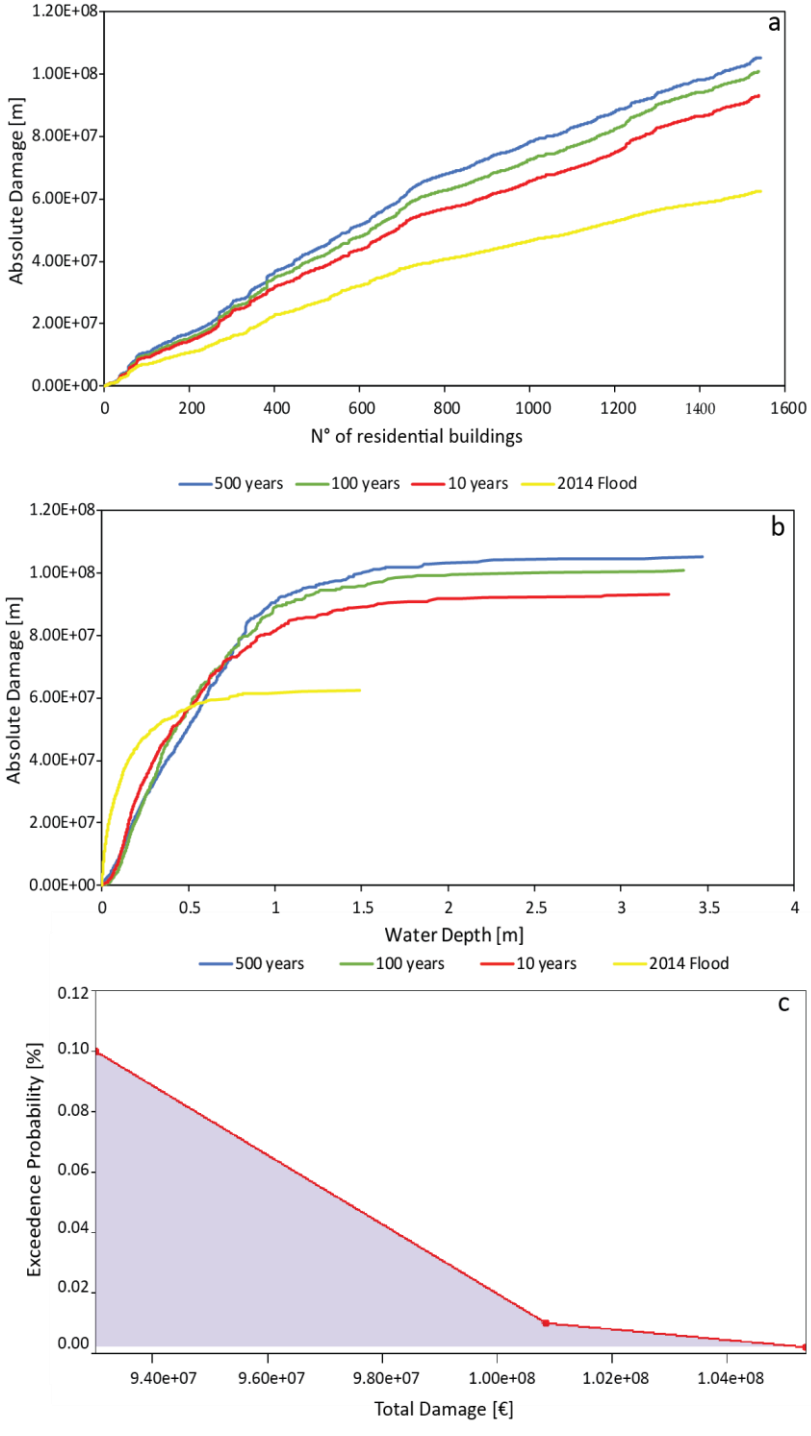

Figure 10: (a) Absolute Damage for the residential sector (n° of buildings) considering 500, 100 and 10 years of return period and the 2014 flood event; (b) Exceedance probability of Absolute Damage for the residential sector; (c) site-specific depth–damage curve for the residential sector considering 500, 100 and 10 years of return period and the 2014 flood event.

https://doi.org/10.5194/egusphere-2022-225
Preprint. Discussion started: 27 April 2022

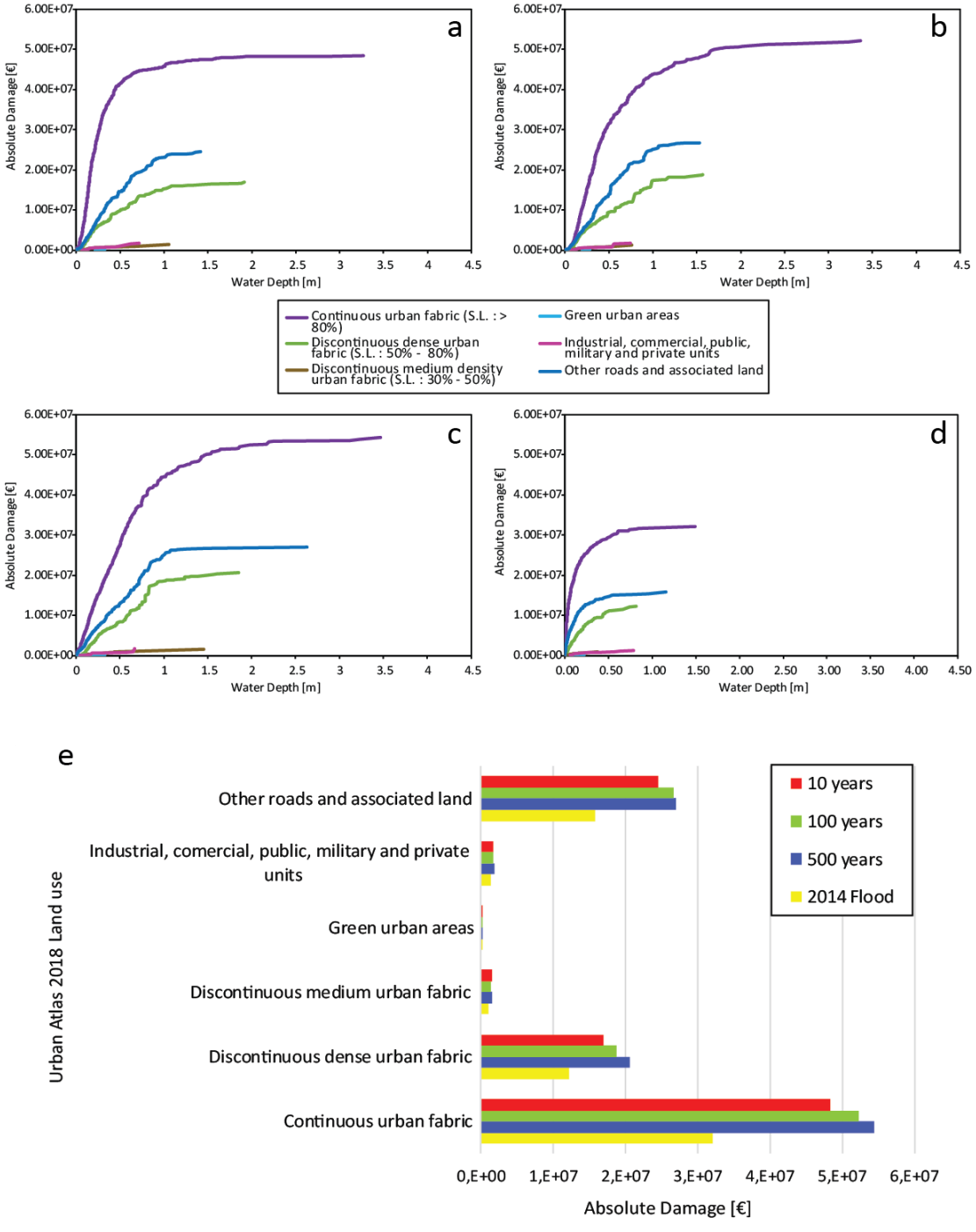

Figure 11: Site-specific mesoscale depth–damage curves for the residential sector. The x-axis represents the inundation depth; the y-axis represents the damage fraction corresponding to the inundation depth for a specific land use class assuming (a) 10, (b) 100, (c) 500 years of return period and (d) 2014 flood. (e) Comparison of total absolute damage distribution at mesoscale.

https://doi.org/10.5194/egusphere-2022-225
Preprint. Discussion started: 27 April 2022

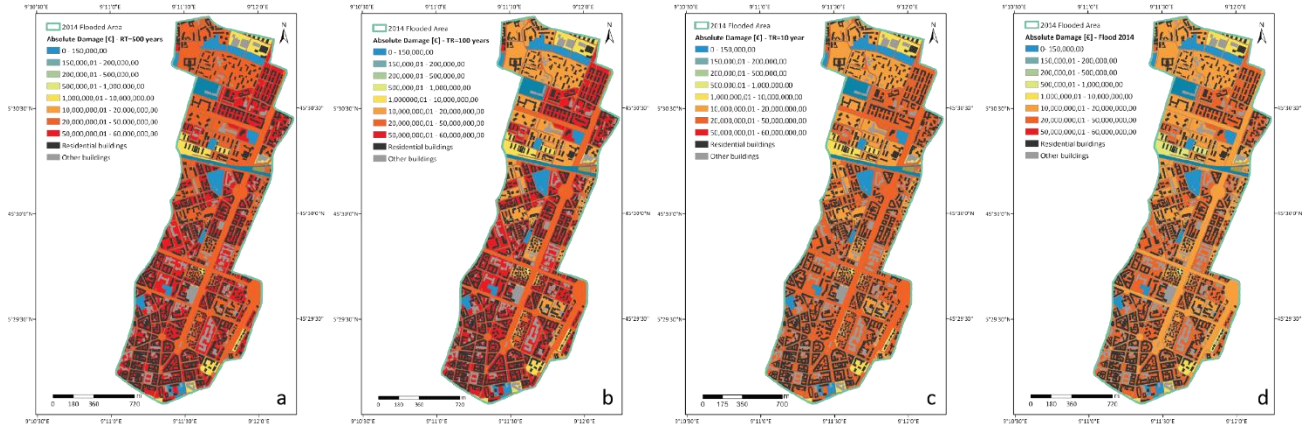

Figure: 12 Mesoscale absolute damage mapping considering (a) 500, (b) 100 and (c) 10 years of return and (d) the 2014 flood event for 2018 Urban Atlas land use classes. Built-up areas shapefile is from © OpenStreetMap contributors 2022. Distributed under the Open Data Commons Open Database License (ODbL) v1.0. Base maps are from © European Union, Copernicus Land Monitoring Service 2022, European Environment Agency (EEA).

https://doi.org/10.5194/egusphere-2022-225
Preprint. Discussion started: 27 April 2022

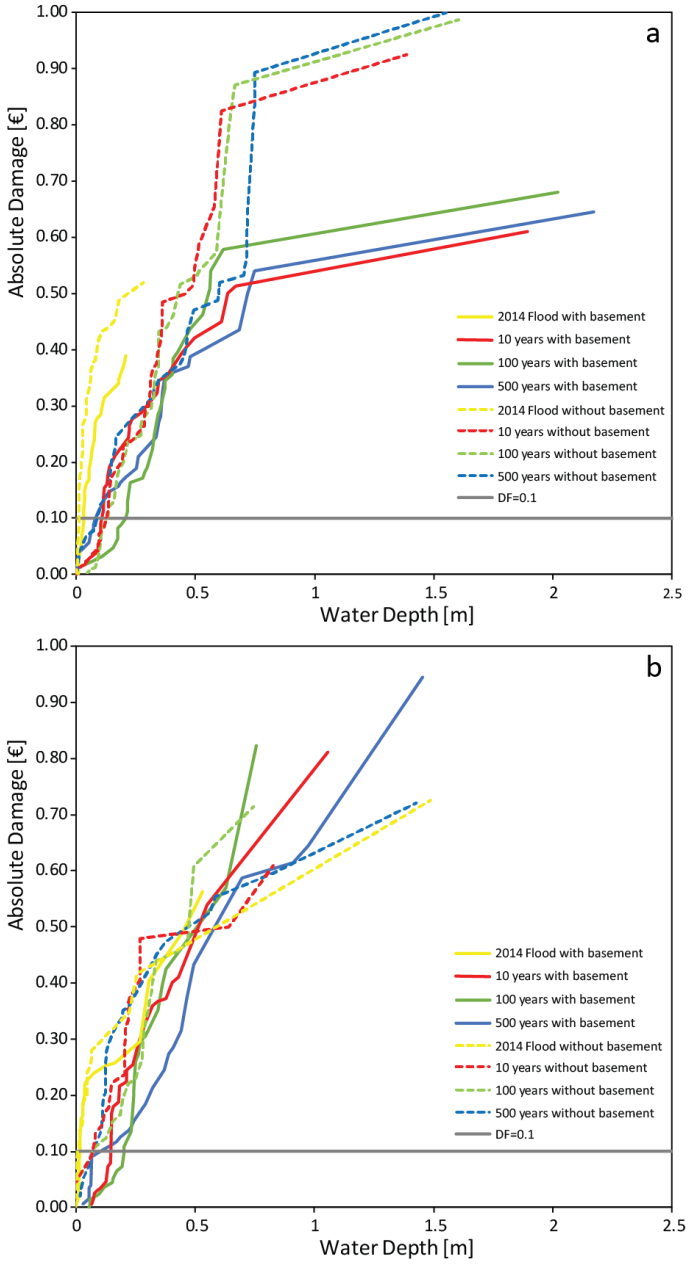

Figure: 13 Site-specific microscale depth–damage curves for the residential sector for the 2014 flood (yellow lines), 10 (red lines), 100 (green lines) and 500 (blue lines) years of return period scenarios for buildings falling in most vulnerable classes (i.e., class 1 and 2, 'Very High' and 'High'): (a) BT='detached and semi-detached house'; MT='masonry'; BS='good'; NISR='0.05-0.12; BH=1-5 m; PC=1919-1966 with basement (solid line) and without basement (dashed lines); (b) BT='detached and semi-detached house'; MT='concrete'; BS='good'; NISR='0.05-0.12; BH=1-5 m; PC=1919-1966 with basement (solid line) and without basement (dashed lines). Solid horizontal grey line stands for DF equal to 0.1.

https://doi.org/10.5194/egusphere-2022-225
Preprint. Discussion started: 27 April 2022

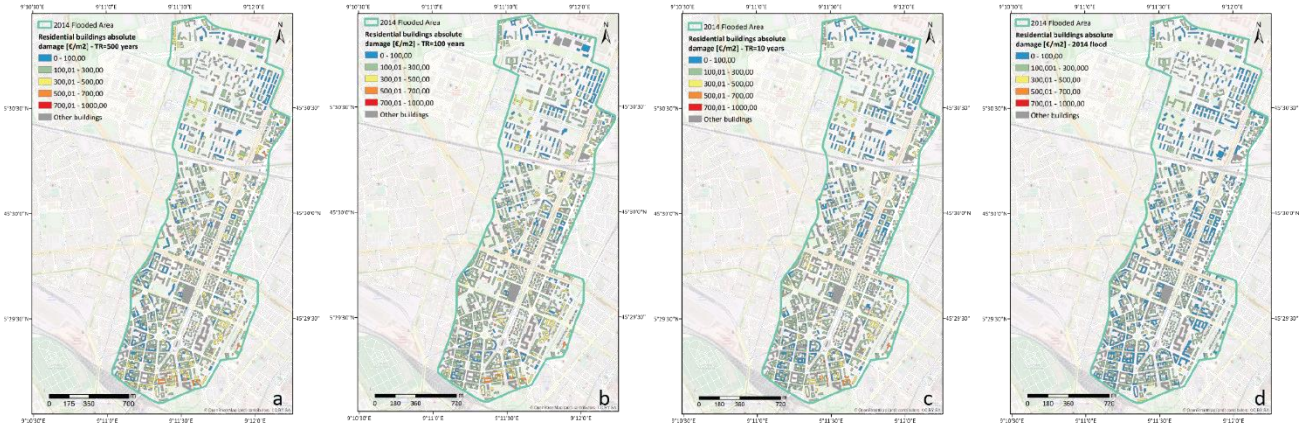

595 **Figure 14: Microscale absolute damage mapping considering (a) 500, (b) 100 and (c) 10 years of return period scenarios and (d) the 2014 flood event for the two most vulnerable building category subsets. Base maps and built-up areas shapefile are from © OpenStreetMap contributors 2022. Distributed under the Open Data Commons Open Database License (ODbL) v1.0.**

Hazard	Class	Weight
Water Depth (WD)	>0.71 m	1
	0.70-0.51 m	2
	0.50-0-31 m	3
	0.30-0.21 m	4
	0.20-0.00 m	5
Sink (SI)	Yes	0
	No	1
Normalized Imperviousness Surface Ratio (NISR)	0.46-1.00	1
	0.46-0.23	2
	0.23-0.12	3
	0.12-0.05	4
	0.05-0.00	5

Table 1: Weights related to Hazard classes for flood depth assigned to residential buildings, on sink map and on NISR classes.

Structural and non-structural feature	Class	Weight	Source
Construction Material Type (MT)	Other material	1	Italian National Institute for Statistics (2011 census, http://www.istat.it/)
	Concrete	2	
	Masonry	3	
Period of construction (PC)	Before 1919	1	Italian National Institute for Statistics (2011 census, http://www.istat.it/)
	1919-1945	2	
	1946-1960	3	
	1961-1970	4	
	1971-1980	5	
	1981-1990	6	
	1991-2000	7	
	2001-2005	8	
	After 2006	9	
	Bad	1	

https://doi.org/10.5194/egusphere-2022-225
Preprint. Discussion started: 27 April 2022

Building Status (BS)	Average	2	Italian National Institute for Statistics (2011 census, http://www.istat.it/)
	Good	3	
	Very Good	4	
Building type (BT)	Detached/semi-detached houses (i.e., dwelling unit inhabited by a single household. Houses forming half of a semi-detached pair)	1	Open Street Maps dataset
	Residential (i.e., building used primarily for residential purposes)	2	
	Apartments (i.e., buildings arranged into individual dwellings, often on separate floors. May also have retail outlets on the ground floor)	3	
Building height (BH)	1-5	1	Italian Ministry of Environment's Geoportale Nazionale (http://wms.pcn.minambiente.it/ogc?map=/msogc/wfs/Edifici.map)
	5-10	2	
	10-15	3	
	15-20	4	
	20-25	5	
	25-30	6	
	30-35	7	
	35-40	8	
	40-100	9	

Table 2: Weights assigned to each structural and feature composing residential buildings, such as MT (i.e., Construction Material Type), PC (i.e., Period of construction), BS (i.e., Building Status), BH (i.e., Building Height), BT (i.e., Building Type).

Total Score	Vulnerability Class
0-17	Very High
18-20	High
21-23	Moderate
24-27	Low
28-34	Very Low

Table 3: Total Score and Vulnerability classes ('Very High', 'High', 'Moderate', 'Low', 'Very Low').

Vulnerability Class	Average economic unit value (€/m²)	Min economic unit value (€/m²)	Max economic unit value (€/m²)
Very Low	3,944.41	2,862.50	10,050.00
Low	3,907.86	1,850.00	10,050.00
Moderate	4,033.10	2,112.50	10,050.00
High	4,065.08	2,112.50	6,200.00
Very High	4,138.20	2,112.50	5,450.00

Table 4: The average, minimum and maximum economic unit value for each residential building structural vulnerability class.

	With basement	No basement

https://doi.org/10.5194/egusphere-2022-225
Preprint. Discussion started: 27 April 2022

Subset	Flood 2014 [m]	10 years scenario [m]	100 years scenario [m]	500 years scenario [m]	Flood 2014 [m]	10 years scenario [m]	100 years scenario [m]	500 years scenario [m]
1	0.03	0.11	0.21	0.08	0.01	0.13	0.12	0.09
2	0.02	0.13	0.20	0.11	0.01	0.07	0.07	0.06

Table 5: Flood depths necessary for causing a DF equal to 0.1, according to the building type two subset.

Appendix

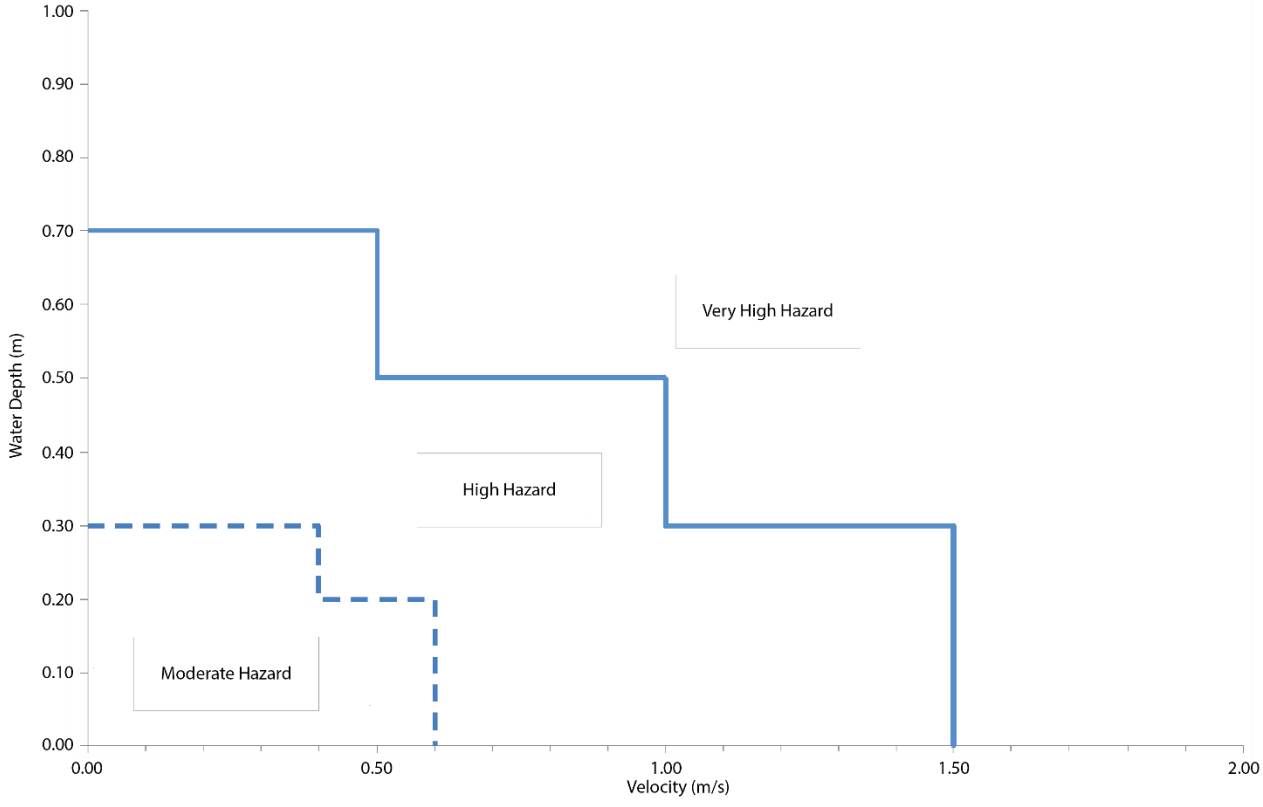

Figure A1: Flood depth and velocity thresholds used as reference values for the flood hazard classification (adapted from Lombardy Region PTC).

Variable	Description	Unit of measurement	Range of values	Default Values	Input Values
he	Water depth outside the building	m	≥0	[0;0.5] Incremental step: 0.01	[0-20.4] Incremental step: 0.05
h	Water depth inside the building (for each floor)	m	[0;1H]	h=f(he, GL)	h=f(he, GL)
v	Max velocity of the water perpendicularly to the building	m/s	≥0	0.5	0.5

https://doi.org/10.5194/egusphere-2022-225
Preprint. Discussion started: 27 April 2022

s	Sediment load	% on the water volume	[0;1]	0.05	0.05
d	Duration of the flood event	hours	>0	24	36
q	Water quality (presence of pollutants)	-	0: No 1: Yes	1	1

Table B1: Features parameters INSYDE model input data.

Variable	Description	Unit of measurement	Range of values	Default Values	Input Values
FA	Footprint area	m^2	>0	100	[11.6; 5400.7]
IA	Internal area	m^2	>0	0.9*FA	0.9*FA
BA	Basement area	m^2	≥0	0.5*FA	0.5*FA
EP	External perimeter	m	>0	4*ξ	[14.1; 895.9]
IP	Internal perimeter	m	>0	2.5 EP	2.5 EP
BP	Basement perimeter	m	>0	4*ξ	4*ξ
NF	Number of floors	-	≥1	2	[1; 4]
IH	Interior floor height	m	>0	3.5	3.5
BH	Basement height	m	>0	3.2	3.2
GL	Ground floor level	m	[-IH;>0]	0.1	0.1
BL	Basement level	m	<0	-GL-BH-0.3	-GL-BH-0.3
BT	Building type	-	1: Detached house 2: Semi-detached house 3: Apartment	1	[1; 2; 3]
BS	Building structure	-	1:reinforced concrete 2: Masonry	2	[1; 2]
FL	Finishing level (i.e., building quality)	-	0.8: low 1:medium 1.2: high	1.2	1.2
LM	Level of maintenance	-	0.9: low 1: medium 1.1: high	1.1	[0.9; 1; 1.1]
YY	Year of construction	-	≥0	1994	[1919; 2006]
PD	Heating system distribution	-	1: centralized 2: distributed	1 if YY≤ 1990 2 otherwise	1 if YY≤ 1990 2 otherwise
PT	Heating system type	-	1: radiator 2: pavement	2 if YY≥ 2000 and FL>1 1 otherwise	2 if YY≥ 2000 and FL>1 1 otherwise

Table B2: Building characteristics parameters INSYDE model input data.

https://doi.org/10.5194/egusphere-2022-225
Preprint. Discussion started: 27 April 2022

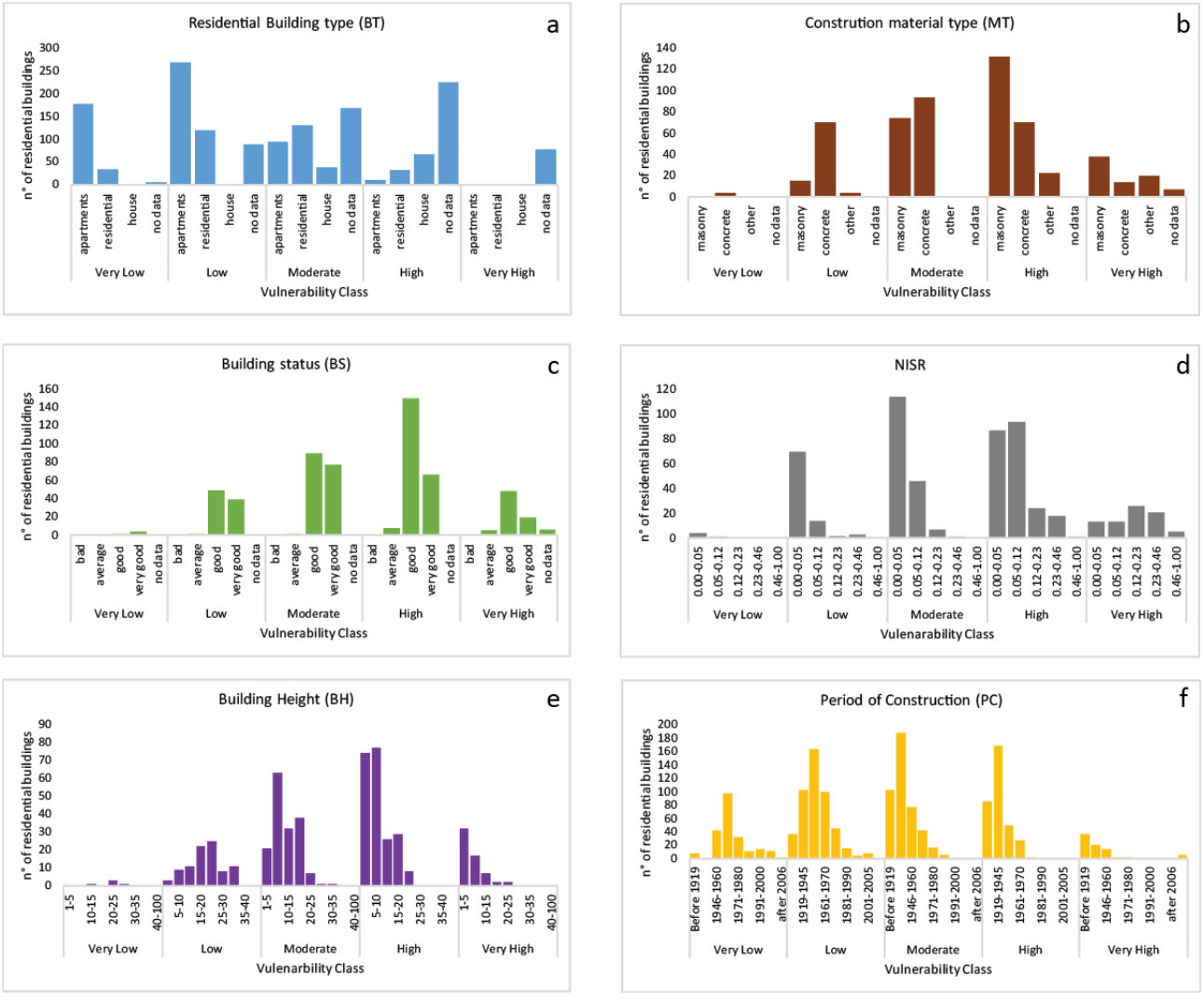

Figure C1: Structural and no structural building characteristics vulnerability class distribution: Residential Buildings Type (a), Construction Material Type (b), Building Status (c), Normalized Imperviousness Surface Ratio) (d), Building Height (e), Period of Construction (f).